Mesoscopic digital control for disturbance string stability via constant time-headway spacing policies

Pietro Bonsanto[1,2], Mattia Mattioni[3], Alessio Iovine[4], Elena De Santis[1] and Maria Domenica Di Benedetto[1]

***Abstract*— This paper addresses the enforcement of Disturbance String Stability (DSS) in connected autonomous vehicle platoons subject to asynchronous communication, sampling, and quantization in case of a constant time headway spacing policy. Building on a mesoscopic control framework, we design digital controllers that guarantee DSS despite external disturbances and device limitations. Simulation results demonstrate the effectiveness of the proposed approach.**

***Index Terms*— Traffic control; Sampled-data control; Autonomous vehicles; String stability; Quantization; Mesoscopic controller; Micro-macro traffic control systems.**

I. Introduction

The transportation landscape has advanced considerably, driven by the demand for efficiency and safety [22, 11, 23]. In this context, intelligent control paradigms such as cooperative adaptive cruise controllers (CACCs), supported by Vehicle-to-Everything (V2X) communications, increase the complexity of ensuring safe behavior in connected autonomous vehicles (CAVs). This work addresses String Stability (SS) [22, 23, 11, 15], i.e., the ability of a platoon to attenuate perturbations as they propagate downstream, and its extension to account for exogenous disturbances, termed Disturbance String Stability (DSS) [3]. Recent studies show that DSS can be achieved through appropriate information exchange, either via leader–follower strategies [3], which rely on pairwise communication and partial leader information, or through Multiple Predecessor Follower (MPF) approaches [1, 25], which employ broader communication among groups of vehicles to compensate for the impracticality of leader information. Similar to the MPF approach, this work avoids relying on the impractical assumption of platoon's leader information by combining *microscopic* quantities, i.e., capturing each vehicle and its predecessor, with *macroscopic* ones, density in particular, that summarize the aggregate state of the platoon. The resulting controller, termed *mesoscopic* [18, 17], leverages both micro- and macro-level information while avoiding the complexity explosion of MPF methods, where the system state grows with the number of vehicles.

Moreover, the proposed control law is designed with realism in mind, accounting for device limitations in signal transmission. In practice, controllers typically developed in an ideal continuous-time framework are implemented via digital devices [28, 21]. The reliance on sampled measurements and piecewise constant inputs significantly affects performance and stability properties of the closed loop, particularly when the sampling frequency is not *sufficiently high* [14, 8]. In addition, measurements are unavoidably subject to quantization, precluding global stability in favor of practical guarantees [10]. Digital effects may even induce instability, such as inter-vehicle gaps and string instability [6, 5]. Yet, few works explicitly address the joint impact of sampling and quantization on SS at the design stage. Building on preliminary results in [13, 4], this work advances in this direction by developing mesoscopic digital controllers that ensure DSS despite sampling, quantization, asynchronous communication, and external disturbances. In particular, we extend the results of [4] to another class of spacing policies, focusing on the *constant time headway spacing policy*. This setting introduces additional complexity: disturbances act through functional terms in the sampled model, and the influence of preceding vehicles becomes non-homogeneous. Consequently, the design of feedback laws enforcing DSS presents methodological challenges beyond those addressed in [4]. Notably, in contrast with most existing works (e.g., [2]), the proposed mesoscopic digital controller guarantees DSS independently of sampling rates, quantization levels, thereby demonstrating the generality of the approach. In addition, all of this is made with no assumption and restriction on the values of the time headway constant, contrary to most works available in the continuous-time concerned literature.

The rest of the paper is organized as follows. Section II provides the models and hypotheses considered, as well as the problem statement. Section III introduces the main result with respect to the aforementioned spacing policy. Section IV shows the effectiveness of the proposed sampled-data quantized solution in simulations, while Section V outlines concluding remarks.

Notations.

$\mathbb{C}$, $\mathbb{N}$ and $\mathbb{R}$ denote the set of complex, natural, and real numbers. $\mathbb{R}^+$ denotes the set of positive real numbers. Given a matrix $A \in \mathbb{R}^{n\times n}$, $\sigma(A) \subset \mathbb{C}$ is its spectrum. A is said to be Schur if its spectrum is included in the open unit circle of the complex plane. $|\cdot| \in \mathbb{R}$ denotes, depending on the

[1] *Università degli Studi dell'Aquila*, Via Vetoio - Coppito, 67100 L'Aquila pietro.bonsanto@student.univaq.it, elena.desantis@univaq.it, mariadomenica.dibenedetto@univaq.

[2] *Polytechnic of Bari, Dept. of Electrical and Information Engineering*, Via Re David 200 70125 Bari-Italy p.bonsanto@phd.poliba.it.

[3] *Dipartimento di Ingegneria Informatica, Automatica e Gestionale A. Ruberti* (Università degli Studi di Roma *La Sapienza*); Via Ariosto 25, 00185 Rome, Italy mattioni@diag.uniroma1.it.

[4] *Laboratoire des Signaux et Systèmes* (L2S), CNRS, CentraleSupélec, Université Paris-Saclay; 3 Rue Joliot Curie, 91190 Gif-sur-Yvette, France alessio.iovine@centralesupelec.fr

argument, either the cardinality of a set $\mathcal{S}$, the absolute value of a complex number $\lambda \in \mathbb{C}$, or the norm of a matrix. Given a set $\mathcal{S}$, we denote by $|\cdot|_{\mathcal{S}}$ the distance between the argument of the modulus and the set $\mathcal{S}$. Given a continuous-time signal $w : \mathbb{R}^+ \mapsto \mathbb{R}$ we define $\|w\|^{[0,\bar{t}]} = \sup_{t\in[0,\bar{t}]} |w(t)|$. For a discrete time signal $w_d : \mathbb{N} \mapsto \mathbb{R}$ we define $||w_d(t_k)||^{[0,\bar{k}]} = \sup_{k\in[0,\bar{k}]} |w_d(t_k)|$. By quantizer, we mean a piecewise constant function $q : \mathbb{R}^n \to \mathcal{R}^n$, with $\mathcal{R}^n$ being a suitable subset of $\mathbb{R}^n$. A quantizer is generally characterized by the parameters D, μ, respectively the range and the quantization error, such that if $|x| \leq D \Rightarrow |q(x)-x| \leq \mu$ with, in addition, $|q(x)| \leq D$ for all $x \in \mathbb{R}^n$ (see [9] and references therein for further details). Along with the aforementioned literature, we assume that D is large enough so that the quantizer never falls into saturation.

II. Modeling and Problem formulation

A. Microscopic modeling

Let $\mathcal{I}_0^N$ be the set of $N+1$ vehicles composing a platoon, including the leader. Each vehicle is described by its longitudinal position, $p_i \in \mathbb{R}^+$, and its longitudinal speed, $0 \leq v_i \leq v_{\max}$, $v_{\max} \in \mathbb{R}^+$, allowing to derive the microscopic dynamics, $\dot{x}_i = \operatorname{col}\left\{v_i, u_i + \tilde{d}_i\right\}$ for all $i \in \mathcal{I}_0^N$, being $\tilde{d}_i$ a disturbance acting on the $i-$th vehicle. For the sake of simplicity (see [23, 27, 7, 12]) and to describe inter-vehicular interactions, we adopt the leader-follower model [19]. In detail, the system incorporates a virtual leader (labeled as $i = -1$) preceding the entire platoon, enabling inclusion of the vehicle $i = 0$. The state of each car-following pair $(i-1, i)$ is defined as $\zeta_i = \operatorname{col}\{\Delta p_i,\ \Delta v_i\}, \quad i \in \mathcal{I}_0^N$ where $\Delta p_i = p_i - p_{i-1}$ and $\Delta v_i = v_i - v_{i-1}$. The microscopic dynamical model reads

$$\dot{\zeta}_i = A\zeta_i + B\left(u_i - u_{i-1} + d_i\right),\ i \in \mathcal{I}_0^N \tag{1}$$

with $u_i, d_i \in \mathbb{R}$ the control input and a bounded disturbance,

$$A = \begin{bmatrix} 0 & 1 \\ 0 & 0 \end{bmatrix}, \quad B = \begin{bmatrix} 0 \\ 1 \end{bmatrix}. \tag{2}$$

The disturbance term $d_i := \tilde{d}_i - \tilde{d}_{i-1}$ aggregates unmodeled effects, including powertrain dynamics, inaccuracies in compensating acceleration signals, and predecessor-follower interactions. As far as the virtual leader is concerned, we assume that it maintains a constant reference speed with no disturbance acting on it.

At this point, at the microscopic level, the problem consists of guaranteeing asymptotic tracking of the time-varying spacing policy

$$\Delta p_i^r = -\Delta\bar{p} - hv_i, \qquad \text{for all } i \in \mathcal{I}_0^N \tag{3}$$

with $\Delta\bar{p}$ the minimum safe distance and $h \in \mathbb{R}^+$ the time headway [26]. The zero speed distance is $-\Delta\bar{p} < 0$. The corresponding equilibrium trajectory $\zeta_{e,i}(t) := \operatorname{col}\{\Delta p_i^r(t), 0\}$ corresponds to vehicles maintaining constant velocity and headway. For design purposes, we introduce coordinate transformation

$$\chi_i = \zeta_i - \zeta_{e,i} = \operatorname{col}\{\Delta p_i + \Delta\bar{p} + hv_i,\ \Delta v_i\} \tag{4}$$

yielding the refined microscopic dynamics

$$\dot{\chi}_i = A\chi_i + B_h\left(u_i - u_{i-1} + d_i\right) + P_h\left(u_{i-1} + \tilde{d}_{i-1}\right) \tag{5}$$

with $B_h = \operatorname{col}\{h, 1\}$ and $P_h = \operatorname{col}\{h, 0\}$ with $\chi_{e,i} = \operatorname{col}\{0, 0\}$. Now, we associate to each vehicle $i \in \mathcal{I}_0^N$, the *microscopic* sampling sequence $\Delta_{\mathtt{m}} = \{t_0, t_1, \ldots, t_k, \ldots\}$ with $T_{\mathtt{m}} = t_{k+1} - t_k > 0$ the microscopic sampling period. At this point, the following assumptions are set.

Assumption 1 (Microscopic Sampling): The input u_i of each vehicle $i \in \mathcal{I}_0^N$ is a piecewise constant signal over the sampling period of length $T_{\mathtt{m}} > 0$; namely,

$$u(t) = u(t_k), \quad t \in [t_k, t_{k+1}), \text{ with } t_k = kT_{\mathtt{m}},\ k \in \mathbb{N}. \tag{6}$$

Under the above assumption, at all sampling instants $t_k = kT_{\mathtt{m}}$ the dynamics of each vehicle (1) is described by the corresponding microscopic sampled-data (equivalent) model, i.e.,

$$\chi_i(t_{k+1}) = A_{\mathtt{d}}\chi_i(t_k) + B_{h,\mathtt{d}}(u_i(t_k) - u_{i-1}(t_k)) + f_i(t_k) \tag{7}$$

with

$$\begin{aligned} A_{\mathtt{d}} &= e^{AT_{\mathtt{m}}} = \begin{bmatrix} 1 & T_{\mathtt{m}} \\ 0 & 1 \end{bmatrix}, \\ B_{h,\mathtt{d}} &= \int_0^{T_{\mathtt{m}}} e^{As}\mathrm{d}sB_h = T_{\mathtt{m}}\begin{bmatrix} \frac{T_{\mathtt{m}}}{2} + h \\ 1 \end{bmatrix}, \\ f_i(t_k) &= \int_0^{T_{\mathtt{m}}} e^{As}\big(B_h d_i(t_{k+1} - s) \\ &\quad + P_h\tilde{d}_{i-1}(t_{k+1} - s)\big)\mathrm{d}s + T_{\mathtt{m}}P_h u_{i-1}(t_k). \end{aligned}$$

Remark 2.1: The model above differs from the one used in [13, 4, 16]. The disturbance term f_i includes a term depending on the inputs of the preceding vehicle, and the model matrices explicitly depend on the constant h associated with the spacing policy.

For control purposes, we now define the measures that are available for the controller design.

Assumption 2 (Microscopic Measurements): Each vehicle $i \in \mathcal{I}_0^N$ measures its corresponding microscopic quantities, i.e., χ_i and u_{i-1}, at all the sampling instants only, which are then subject to quantization.

B. Macroscopic modeling

In a real-traffic scenario, each vehicle $i \in \mathcal{I}_0^N$ experiences influences from its immediate predecessor and reacts to them according to the state of the traffic ahead, that is, on the platoon interactions [24, p. 353]. The former information is embedded in the microscopic measurements (defined in the previous section), whereas the latter is here synthetized in the so-called *macroscopic function*

$$\psi_{i-1}(\chi_0, \cdots, \chi_{i-1}) : \mathbb{R}^2 \times \cdots \times \mathbb{R}^2 \to \mathbb{R}^2 \tag{8}$$

satisfying, for all $i \in \mathcal{I}_0^N$

$$|\psi_{i-1}(\chi_0, \cdots, \chi_{i-1})| \leq c \max_{i\in\mathcal{I}_0^N} |\chi_{i-1}|, \tag{9}$$

with some constant $c \in \mathbb{R}^+$ and $\psi_{i-1}(\chi_{e,1}, \chi_{e,2}, \cdots, \chi_{e,i}) = \operatorname{col}\{0, 0\}$. We express macroscopic information in terms of microscopic variables, inspired by the link between macroscopic traffic density and microscopic variance of distances and speed differences described in [24]. Therefore, Eq. (8) is concerned with macroscopic density. Moreover, condition (9) depicts the realistic situation where density stays finite. In practice, density cannot exceed a maximum threshold, commonly defined as traffic jam density. Referring to infinite density would portray a scenario where vehicles are infinitely close together, which is unfeasible since each vehicle has a finite length.

As one would expect, the macroscopic quantities are available to each vehicle at sporadic and intermittent time instants, and are subject to quantization. To endow this into the design model, we denote the macroscopic sampling sequence by $\Delta_{\mathtt{M}} = \{t_{0^{\mathtt{M}}}, t_{1^{\mathtt{M}}}, \cdots, t_{k^{\mathtt{M}}}, \cdots\} \subseteq \Delta_{\mathtt{m}}$ with $t_{k^{\mathtt{M}}+1} - t_{k^{\mathtt{M}}} = MT_{\mathtt{m}}$ for $M \in \mathbb{N} \setminus \{0\}$.

Assumption 3 (Macroscopic Sampling): Each vehicle $i \in \mathcal{I}_0^N$ receives the quantized macroscopic information function (8) at all $t_{k^{\mathtt{M}}} \in \Delta_{\mathtt{M}}$ with corresponding macroscopic sampling period $T_{\mathtt{M}} := MT_{\mathtt{m}} = t_{k^{\mathtt{M}}+1} - t_{k^{\mathtt{M}}}$ for some $M \in \mathbb{N} \setminus \{0\}$.

We highlight that macroscopic and microscopic measurements are asynchronous, thus reflecting the delay in transmission related to V2I communication, in contrast with quicker V2V ones, enabled by onboard sensors.

C. Problem statement

Given the assumptions 1 to 3, let us consider a piecewise constant feedback law $u_i(t_k)$ that asymptotically tracks the desired distance and velocity profile using asynchronous micro and macroscopic information, to ensure a desired behavior under quantized and sampled-data measurements. By desired behavior, we mean that the closed-loop platoon is practically and disturbance string stable, as defined below. Let the controller $u_i(t_k)$ be of the form

$$u_i(t_k) = u_{i-1}^q(t_k) - K_{\mathtt{d}}\chi_i^q(t_k) + R_{\mathtt{d}}\psi_{i-1}^q(t_{k^{\mathtt{M}}}), \tag{10}$$

with $u_{i-1}^q(t_k) := q(u_{i-1}(t_k))$, $\chi_i^q(t_k) = q(\chi_i(t_k))$, $\psi_{i-1}^q(t_{k^{\mathtt{M}}}) = \psi_{i-1}(q(\chi_{i-1}(t_{k^{\mathtt{M}}})))$, $K_{\mathtt{d}}, R_{\mathtt{d}} \in \mathbb{R}^{1\times 2}$, making $\chi_e = \operatorname{col}\{0,0\}$. Let us consider the closed loop system (7)-(10).

Definition 2.1 (Practical String Stability , pSS): For all $i \in \mathcal{I}_0^N$, considering $d_i \equiv \tilde{d}_i \equiv 0$, the closed loop system is said to be *practically string stable* if there exists $\vartheta_\mu \geq 0$ such that the following conditions hold for all $N \in \mathbb{N}$:

(i) for all $\varepsilon > 0$ there exists $\alpha_\varepsilon > 0$ such that, for all $t_k \in \Delta_{\mathtt{m}}$

$$\max_{i\in\mathcal{I}_0^N} |\chi_i(0)| < \alpha_\varepsilon \Rightarrow \max_{i\in\mathcal{I}_0^N} |\chi_i(t_k)| < \varepsilon + \vartheta_\mu; \tag{11}$$

(ii) the trajectories asymptotically approach the set $\mathcal{B}_{\vartheta_\mu}(\chi) = \{\chi \in \mathbb{R}^2 : |\chi| \leq \vartheta_\mu\}$, i.e.,

$$\lim_{t_k\to\infty} |\chi_i(t_k)|_{\mathcal{B}_{\vartheta_\mu}} = 0. \tag{12}$$

Besides quantization, to cope with the presence of exogenous perturbations, we consider this definition based on [3]:

Definition 2.2 (Disturbance practical String Stability, DSS): For all $i \in \mathcal{I}_0^N$, the origin of the closed loop system is said to be *disturbance practically string stable* under quantization if there exist functions β_d of class $\mathcal{KL}$, ρ_d of class $\mathcal{K}_\infty$ and constants $\delta > 0, \delta_d > 0$ such that, for any initial condition $\chi_i(0)$ and disturbance d_i satisfying

$$\max\nolimits_{i\in\mathcal{I}_0^N} |\chi_i(0)| \leq \delta,\ \max\nolimits_{i\in\mathcal{I}_0^N} |d_i(t_k)|^{[0,t_k]} < \delta_d \tag{13}$$

the solution $\chi_i(t_k)$ exists for all $t_k \geq 0$, and satisfies, for all $N \in \mathbb{N}$,

$$\max_{i\in\mathcal{I}_0^N} |\chi_i(t_k)|_{\mathcal{B}_{\vartheta_\mu}} \leq \beta_d(\max_{i\in\mathcal{I}_0^N} |\chi_i(0)|, t_k) + \rho_d(\max_{i\in\mathcal{I}_0^N} |d_i|^{[0,t_k]}).$$

In this sense, the problem we address concerns the design of a digital control law simultaneously enforcing DSS in presence of exogenous perturbations and pSS with respect to quantization, as stated below.

Disturbance And Practical String Stability Under Quantization Digital Control Problem (qDSS-DCP): Consider a platoon of vehicles described by (1), under Assumptions 1, 2 and 3 with the macroscopic information (8) verifying (9). The equilibrium $\chi_e = \operatorname{col}\{0,0\}$ of the closed-loop system (7)-(10) is Disturbance String Stable under quantization (qDSS) if the following properties hold:

$i)$ pSS with respect to quantization in the sense of Def. 2.1;
$ii)$ DSS with respect to d_i in the sense of Def. 2.2. ▲

The controller (10) relies solely on asynchronous, quantized, and sampled measurements. It consists of two main parts: the first two addends represent macro-information available at all vehicles at the microscopic sampling instants, while the last one represents the macro-information available at the corresponding sampling instants. This information is shared via V2X communications, as seen in [20].

Remark 2.2: Both Def. 2.1 and Def. 2.2 and the inequalities therein are independent on the choices of the quantizer parameters μ, D, the asynchronism scaling factor and the microscopic sampling period M, T_m and time headway h.

III. Control Design

The problem is solved by modelling the effect of quantization as an endogenous perturbation in the sampled equivalent model (7). DSS is ensured with respect to both disturbances, and qDSS is attained by separating the quantization component. The main result is stated in the following, with the proof in the Appendix.

Theorem 3.1: The *qDSS-DCP* is solved by the control (10) with $\psi_{i-1}(t_{k^{\mathtt{M}}})$ as in (8), provided that the matrices $K_{\mathtt{d}}$ and $R_{\mathtt{d}}$ fulfill the conditions below:

1) the matrix $F_{\mathtt{d}} = A_{\mathtt{d}} - B_{h,\mathtt{d}}K_{\mathtt{d}}$ is Schur;
2) for some $M \in \mathbb{N} \setminus \{0\}$ the parameter

$$\begin{aligned}\gamma(\alpha,\beta,r,\kappa,h) = \beta(1-\alpha)^{-1}\Big(&b_h cr(1+\beta\alpha^M)(1-\alpha)^{-1} \\ &+ b_h cr(1+\beta+hT_{\mathtt{m}}) + T_{\mathtt{m}}h\kappa\Big)\end{aligned} \tag{14}$$

with $\alpha \in (0,1)$ and $\beta \geq 0$ such that $|F_{\mathtt{d}}^k| \leq \beta\alpha^k$ for all $k \in \mathbb{N}$, $r = |R_{\mathtt{d}}|$, $\kappa = |K_{\mathtt{d}}|$, $b_h = |B_{h_{\mathtt{d}}}| = T_m\sqrt{1+(T_{\mathtt{m}}/2+h)^2}$ verifies $\gamma(\alpha,\beta,r,\kappa,h) \in (0,1)$.

Then, the control law (10) ensures qDSS for the platoon of vehicles (7) in the sense of Def. 2.1 and Def. 2.2, with $\rho_d(s) = \vartheta_d s$, and

$$\begin{aligned}\vartheta_d &= (\tilde{\alpha}\tilde{\gamma})^{-1}\left(\beta b_h(2b_h + hT_{\mathtt{m}})\right) \\ \vartheta_\mu &= (\tilde{\alpha}\tilde{\gamma})^{-1}\beta b_h(b_h + hT_{\mathtt{m}})\Big(\mu(\kappa+r) + hT_{\mathtt{m}}D\Big)\end{aligned} \tag{15}$$

with $\tilde{\alpha} = (1-\alpha)$ and $\tilde{\gamma} = (1-\gamma)$.

Remark 3.1: The parameter (14) depends on α, β, r, κ, and h, which the designer can set. For a fixed sampling rate $T_{\mathtt{m}}$, DSS can be achieved by balancing regulation (via α, β) and time headway policy constraints (via h).

IV. Numerical Results

In this section, we consider a platoon of $N = 9$ vehicles plus the leader. The choice for the minimum safe distance is $\Delta\bar{p} = 20\ m$ while $h = 0.1$, with initial desired speed of the leader of $20\ m/s$. Moreover, we saturate the control for each vehicle by $|u_i| \leq 5\ m/s^2$. The simulation time is $60s$. The

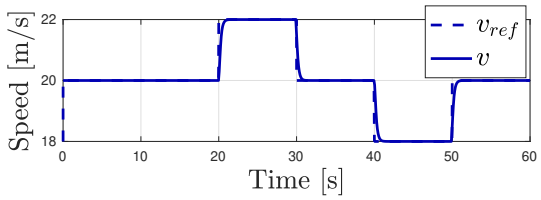

Fig. 1: Speed of the leader and tracked reference.

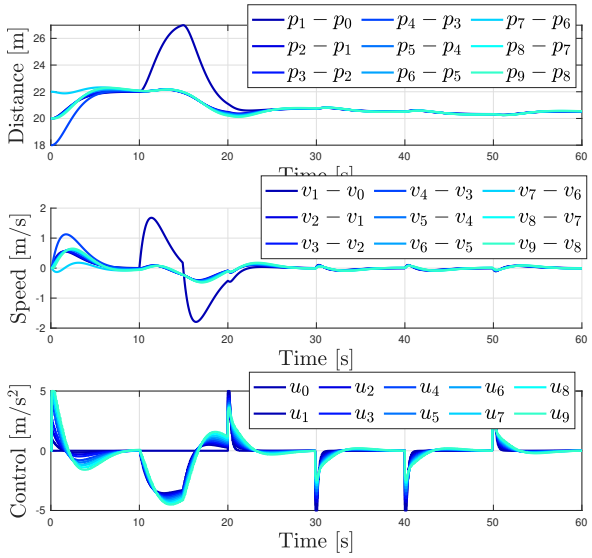

(a) The distance, velocity difference and control inputs .

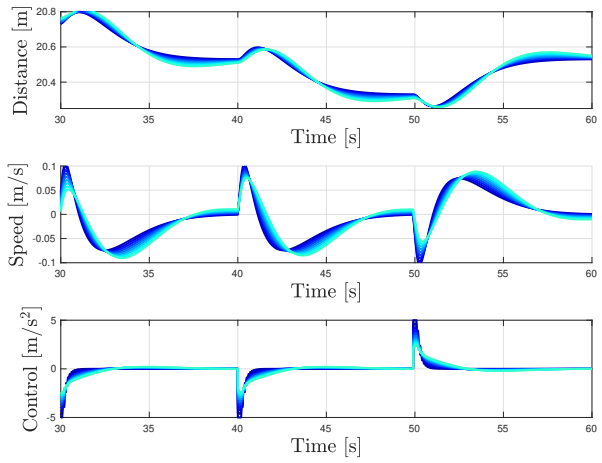

(b) Zoom of Fig. 2a between $t = 30\ s$ and $t = 60\ s$.

construction of the macroscopic functions presented in Section II-B follows the same procedure presented in previous works (see [4, 16]). More in detail, for all $i \in \mathcal{I}_0^N$ and omitting the function arguments, we define for $l \in \{\Delta p, \Delta v\}$

$$\mu_{l,i-1} := \frac{1}{i}\sum_{j=0}^{i-1} l_j,\ \ \sigma^2_{l,i-1} := \frac{1}{i}\sum_{j=0}^{i-1}(l_j - \mu_{l,i-1})^2, \qquad (16)$$

computed from vehicle 0 to vehicle $i-1$.

Then, the macroscopic function (8) is given by $\psi_{i-1} = \begin{bmatrix}\psi^{\Delta p}_{i-1} & \psi^{\Delta v}_{i-1}\end{bmatrix}^\top$, with the components being

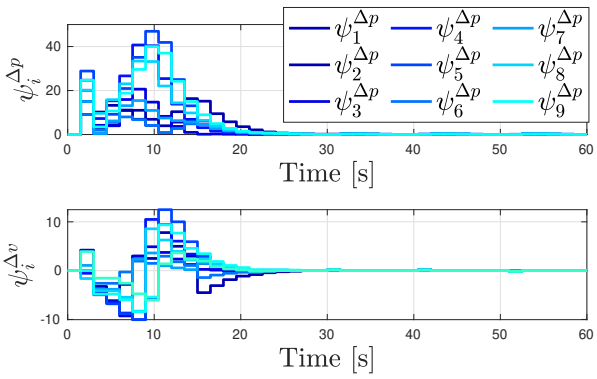

Fig. 3: Macroscopic information function.

$$\psi^l_{i-1} = \text{sign}(\mu_{l,i-1} - \bar{\chi}_l)\sqrt{\sigma^2_{l,i-1}}, l \in \{\Delta p, \Delta v\} \qquad (17)$$

with $\bar{\chi}_{\Delta p} = -\Delta\bar{p}$ and $\bar{\chi}_{\Delta v} = 0$.

The platoon leader is fed with a piecewise constant reference profile $v_{ref}(t)$, as noticeable inspecting Fig. 1. In opposition, with reference to the disturbance acting on the platoon, we assume the simulation time to be divided into distinct phases: 1) for $t \in [0, 10) \cup [15, 20) \cup [25, 40) \cup [50, 60]$, no disturbance is acting over, i.e., $d_i(t) \equiv 0$ for all $i \in \mathcal{I}_0^{10}$; 2) for $t \in [10, 15)s$, a constant disturbance $d_1(t) = 3$ acts on the first vehicle only; 3) for $t \in [20, 25)s$ a constant disturbance $d_1(t) = -3$ acts on the first vehicle; 4) for $t \in [40, 50)s$, a sinusoidal disturbance is acting on each vehicle of the platoon. The microscopic sampling period is chosen as $T_{\mathtt{m}} = 0.1$s and the macroscopic one is $T_{\mathtt{M}} = 1.5$s, hence, $M = 15$. This choice results in $\gamma = 2 \cdot 10^{-4}$. In Figs. 2a-2b, we provide the plots for the distances, speed differences, and control inputs for each vehicle in the platoon, thus adopting the constant time-headway spacing policy. Looking at the first figure, we can see the harmonization in the transient phase achieved incrementally for each vehicle, as we move towards the end of the platoon, via the use of the macroscopic information. This is not surprising, since such a harmonizing effect was well inspected in [18], hinting that a traffic-aware controller could, in principle, enhance the transient phase. This is reflected in the proposed simulation, since the tailing vehicles experience no overshooting, compared with the previous ones. Another important aspect is that the disturbance acting does not amplify, but rather they are attenuated towards the trailing vehicles, proving the achievement of DSS. Inspecting Fig. 2b, which zooms in on Fig. 2a between $t = 30$ s and $t = 60$ s, one can observe the achievement of the pSS property. At the instants when the leader reference changes, each vehicle experiences perturbations that persist due to the mismatch between past control actions and their quantized values used in the controller. The resulting perturbation could, in principle, propagate, thus violating the desired properties. Nonetheless, the proposed controller succeeds in enforcing pSS, that is noticed by the offset the trajectory converges with, deviating from the expected distance. Indeed, the proposed choice for h would lead to an equilibrium of 22 m, which is not the case since the quantized controller induces an offset that implies a different equilibrium. Regardless, performances are still satisfactory, proving both DSS and pSS. Again, the

estimate of ϑ_μ is quite conservative; thus, the offset can be different depending on the case. In the same figure, one can easily see how the tracked distance changes depending on how the velocity for each vehicle changes, thanks to the specific spacing policy. At last, in Fig.3 we provide the plot for the macroscopic information hereby considered, both computed with respect to distance and speed. Thus, as the definition suggests, such a function vanishes when the platoon reaches its equilibrium.

V. Conclusion

We presented a digital mesoscopic controller that enforces DSS and pSS in a vehicle platoon while mitigating the effects of quantization, sampling, and asynchronous communication. The design relies on a novel platoon model implementing a constant time headway spacing policy. Future work will focus on reducing the information required by each vehicle, making the macroscopic function dependent only on a subset of preceding vehicles.

References

[1] E. Abolfazli, B. Besselink, and T. Charalambous. "Minimum time headway in platooning systems under the MPF topology for different wireless communication scenario". In: *IEEE Trans. on Intelligent Transportation Systems* 24.4 (2023), pp. 4377–4390.

[2] E. Abolfazli, B. Besselink, and T. Charalambous. "On time headway selection in platoons under the MPF topology in the presence of communication delays". In: *IEEE Transactions on Intelligent Transportation Systems* 23.7 (2021), pp. 8881–8894.

[3] B. Besselink and K. H. Johansson. "String Stability and a Delay-Based Spacing Policy for Vehicle Platoons Subject to Disturbances". In: *IEEE Transactions on Automatic Control* 62.9 (2017), pp. 4376–4391.

[4] P. Bonsanto, M. Mattioni, A. Iovine, E. De Santis, and M. D. Di Benedetto. "Mesoscopic digital control for Practical String Stability of vehicular platoons". In: *2024 IEEE 63rd Conference on Decision and Control (CDC)*. 2024, pp. 5705–5710.

[5] S. Cui, Y. Xue, M. Lv, K. Gao, B. Yu, and J. Cao. "Temporal Finite-Time Adaptation in Controlling Quantized Nonlinear Systems Amidst Time-Varying Output Constraints". In: *IEEE Transactions on Automation Science and Engineering* 22 (2025), pp. 3265–3279.

[6] S. Cui, Y. Xue, M. Lv, B. Yao, and B. Yu. "Cooperative Constrained Control of Autonomous Vehicles With Nonuniform Input Quantization". In: *IEEE Transactions on Vehicular Technology* 71.11 (2022), pp. 11431–11442.

[7] M. di Bernardo, A. Salvi, and S. Santini. "Distributed Consensus Strategy for Platooning of Vehicles in the Presence of Time-Varying Heterogeneous Communication Delays". In: *IEEE Trans. on Intelligent Transportation Systems* 16.1 (2015).

[8] M. Di Ferdinando and P. Pepe. "Sampled-data emulation of dynamic output feedback controllers for nonlinear time-delay systems". In: *Automatica* 99 (2019), pp. 120–131.

[9] M. Di Ferdinando, P. Pepe, and A. Borri. "On practical stability preservation under fast sampling and accurate quantization of feedbacks for nonlinear time-delay systems". In: *IEEE Transactions on Automatic Control* 66.1 (2020), pp. 314–321.

[10] M. Di Ferdinando, P. Pepe, and E. Fridman. "Practical stability preservation under sampling, actuation disturbance and measurement noise, for globally lipschitz time-delay systems". In: *Accounting for Constraints in Delay Systems*. Springer, 2022, pp. 109–124.

[11] S. Feng, Y. Zhang, S. E Li, Z. Cao, H. X. Liu, and L. Li. "String stability for vehicular platoon control: Definitions and analysis methods". In: *Annual Reviews in Control* 47 (2019), pp. 81–97.

[12] V. Giammarino, S. Baldi, P. Frasca, and M. L. Delle Monache. "Traffic Flow on a Ring With a Single Autonomous Vehicle: An Interconnected Stability Perspective". In: *IEEE Transactions on Intelligent Transportation Systems* 22.8 (2021).

[13] A. Iovine, M. Mattioni, and G. Tedeschi. "Sampled-data String Stability for a Platoon of heterogeneous vehicles via a mesoscopic approach". In: *2024 European Control Conference (ECC)*. 2024, pp. 3364–3369.

[14] I. Karafyllis and C. Kravaris. "Global stability results for systems under sampled-data control". In: *International Journal of Robust and Nonlinear Control* 19.10 (2009), pp. 1105–1128.

[15] H. Li, Y. Shi, and W. Yan. "Distributed receding horizon control of constrained nonlinear vehicle formations with guaranteed γ-gain stability". In: *Automatica* 68 (2016), pp. 148–154.

[16] M. Mattioni and A. Iovine. "Asynchronous Sampled-Data String Stability for a Platoon of Heterogeneous Vehicles via a Mesoscopic Approach". In: *IEEE Transactions on Control Systems Technology* 33.4 (2025), pp. 1345–1360.

[17] M. Mirabilio, A. Iovine, E. De Santis, M. D. Di Benedetto, and G. Pola. "Mesoscopic controller for string stability of platoons with disturbances". In: *IEEE Transactions on Control of Network Systems* 9.4 (2022), pp. 1754–1766.

[18] M. Mirabilio, A. Iovine, E. De Santis, M. D. Di Benedetto, and G. Pola. "String stability of a vehicular platoon with the use of macroscopic information". In: *IEEE Transactions on Intelligent Transportation Systems* 22.9 (2021), pp. 5861–5873.

[19] J. Ploeg, N. van de Wouw, and H. Nijmeijer. "$\mathcal{L}_p$ String Stability of Cascaded Systems Application to Vehicle Platooning". In: *IEEE Transactions on Control Systems Technology* 22.2 (2014), pp. 786–793.

[20] L. Prade Njoua Dongmo, J. Auriol, and A. Iovine. "Smart Traffic Manager for Speed Harmonization and Stop-and-Go Waves Mitigation Dedicated to Connected Autonomous Vehicles". In: *IEEE Transactions on Control Systems Technology* 33.4 (2025), pp. 1447–1462.

[21] Z. Shen, Y. Liu, Z. Li, and M. H. Nabin. "Cooperative spacing sampled control of vehicle platoon considering undirected topology and analog fading networks". In: *IEEE Transactions on Intelligent Transportation Systems* 23.10 (2022), pp. 18478–18491.

[22] R. E. Stern, S. Cui, M. L. Delle Monache, R. Bhadani, M. Bunting, M. Churchill, N. Hamilton, H. Pohlmann, F. Wu, B. Piccoli, et al. "Dissipation of stop-and-go waves via control of autonomous vehicles: Field experiments". In: *Transportation Research Part C: Emerging Technologies* 89 (2018), pp. 205–221.

[23] D. Swaroop and J. K. Hedrick. "String stability of interconnected systems". In: *IEEE transactions on automatic control* 41.3 (1996), pp. 349–357.

[24] M. Treiber and A. Kesting. "Traffic flow dynamics". In: *Traffic Flow Dynamics: Data, Models and Simulation, Springer-Verlag Berlin Heidelberg* (2024), pp. 983–1000.

[25] P. Wijnbergen and B. Besselink. "Existence of decentralized controllers for vehicle platoons: On the role of spacing policies and available measurements". In: *Systems & Control Letters* 145 (2020), p. 104796.

[26] C. Wu, Z. Xu, Y. Liu, C. Fu, K. Li, and M. Hu. "Spacing policies for adaptive cruise control: A survey". In: *IEEE Access* 8 (2020), pp. 50149–50162.

[27] L. Xiao and F. Gao. "Practical String Stability of Platoon of Adaptive Cruise Control Vehicles". In: *IEEE Trans. on Intelligent Transportation Systems* 12.4 (2011), pp. 1184–1194.

[28] P. Zhu, S. Jin, X. Bu, and Z. Hou. "Distributed data-driven control for a connected heterogeneous vehicle platoon under quantized and switching topologies communication". In: *IEEE Transactions on Vehicular Technology* 72.8 (2023), pp. 9796–9807.

Appendix
Proof of Theorem 3.1

The closed-loop platoon reads as the cascade

$$\chi_i(t_{k+1}) \quad = F_{\mathtt{d}}\chi_i(t_k) + G_{\mathtt{d}}\psi_{i-1}(t_{k^{\mathtt{M}}}) + w_i(t_k), \quad i \in \mathcal{I}_0^N$$

with $\psi_0(t_{k^{\mathtt{M}}})=0$,

$$\begin{aligned} w_i(t_k) = \; & f_i(t_k) + B_{h,\mathtt{d}} K_{\mathtt{d}} \left(\chi_i^q(t_k) - \chi_i(t_k)\right) \\ & + G_{\mathtt{d}} \left(\psi_{i-1}^q(t_{k^{\mathtt{M}}}) - \psi_{i-1}(t_{k^{\mathtt{M}}})\right) \\ & + B_{h,\mathtt{d}} \left(u_{i-1}^q(t_k) - u_{i-1}(t_k)\right) \end{aligned}$$

and $w_0(t_k) = f_0(t_k) + B_{h,\mathtt{d}} K_{\mathtt{d}} (\chi_0^q(t_k) - \chi_0(t_k))$. The term above is composed of $f_i(t_k)$, the actual exogenous perturbation, and the one induced by quantization errors associated to each signal. Keeping in mind that $t_k = kT_{\mathtt{m}} \in \Delta_m$, $t_{k^{\mathtt{M}}} = k^{\mathtt{M}} M T_{\mathtt{m}} \in \Delta_M$ and $t_{k^{\mathtt{M}}} \leq t_k$, one can rewrite $k = Mk^{\mathtt{M}} + \bar{k}$, $\bar{k} \in \{0, 1, \cdots, M-1\}$. Accordingly, the explicit dynamics of each vehicle reads

$$\begin{aligned} \chi_i(t_k) = F_{\mathtt{d}}^k \chi_i(0) + \textstyle\sum_{l=0}^{k} F_{\mathtt{d}}^{(k-1-l)} w_i(t_l) + \boldsymbol{F_{\bar{k}}} G_{\mathtt{d}} \psi_{i-1}(t_{k^{\mathtt{M}}}) \\ + \boldsymbol{F_M} \textstyle\sum_{l=0}^{k^{\mathtt{M}}} F_{\mathtt{d}}^{k^{\mathtt{M}}-(l+1)M} G_{\mathtt{d}} \psi_{i-1}(t_l) \end{aligned} \tag{18}$$

where $\boldsymbol{F_\ell} = (I - F_{\mathtt{d}})^{-1}(I - F_{\mathtt{d}}^\ell)$ for $\ell \in \{M, \bar{k}\}$. We proceed iteratively and by induction by considering the platoon composed of the virtual leader and the first vehicle (i.e., $i=0$ and $i=1$) at first. By condition 1), the matrix $F_{\mathtt{d}}$ is Schur stable and there exist $\beta > 0$ and $\alpha \in (0,1)$ such that $|F_{\mathtt{d}}^k| \leq \beta\alpha^k$ yielding

$$|\chi_0(t_k)| \leq \beta\alpha^k |\chi_0(0)| + \beta\tilde{\alpha}^{-1} \|w_0(t_\ell)\|^{[0,k]}. \tag{19}$$

As far as $i=1$ is concerned, keeping in mind the form (18) and that $|F_{\mathtt{d}}^k| \leq \beta\alpha^k$, one gets

$$\begin{aligned} |\chi_1(t_k)| \; & \leq \beta\alpha^k |\chi_1(0)| + \beta\tilde{\alpha}^{-1} \|w_1(t_\ell)\|^{[0,k]} \\ & + \beta b_h r \tilde{\alpha}^{-2} (1 + \beta\alpha^M) \|\psi_0(t_\ell)\|^{[0,k^{\mathtt{M}}]} \\ & + \beta b_h r \tilde{\alpha}^{-1} (1 + \beta\alpha^k) \|\psi_0(t_\ell)\|^{[0,k^{\mathtt{M}}]} \end{aligned}$$

for $\tilde{\alpha} = 1 - \alpha > 0$. At this point, (9) implies $\|\psi_0(\chi_0(t_\ell))\|^{[0,k^{\mathtt{M}}]} \leq c\|\chi_0(t_\ell)\|^{[0,k^{\mathtt{M}}]} \leq c\|\chi_0(t_\ell)\|^{[0,k]}$ that, combined with (19), yields

$$\begin{aligned} |\chi_1(t_k)| \; & \leq \beta\alpha^k |\chi_1(0)| + \beta\tilde{\alpha}^{-1} \|w_1(t_\ell)\|^{[0,k]} \\ & + c\beta b_h r \tilde{\alpha}^{-2} (1 + \beta\alpha^M) \|\chi_0(t_\ell)\|^{[0,k]} \\ & + c\beta b_h r \tilde{\alpha}^{-1} (1 + \beta) \|\chi_0(t_\ell)\|^{[0,k]}. \end{aligned}$$

Since the terms $f_1(t_k)$ and $w_1(t_k)$ are such that

$$\begin{aligned} \|f_1(t_k)\|^{[0,k]} & \leq (2b_h + hT_{\mathtt{m}})\delta_d + T_{\mathtt{m}} h \|u_0(t_\ell)\|^{[0,k]} \\ & \leq (2b_h + hT_{\mathtt{m}})\delta_d + \kappa T_{\mathtt{m}} h \left(\mu + \|\chi_0(t_\ell)\|^{[0,k]}\right), \\ \|w_1(t_k)\|^{[0,k]} & \leq (2b_h + hT_{\mathtt{m}})\delta_d + \kappa T_{\mathtt{m}} \left(\mu + h\|\chi_0(t_\ell)\|^{[0,k]}\right) \\ & \quad + b_h \kappa \mu. \end{aligned}$$

where μ is the quantization error. By definition of (14), the following inequality holds true

$$\begin{aligned} |\chi_1(t_k)| \; & \leq \beta\alpha^k |\chi_1(0)| + \beta\tilde{\alpha}^{-1} (2b_h + hT_{\mathtt{m}})\delta_d \\ & + \beta\tilde{\alpha}^{-1} b_h \kappa\mu + \beta\tilde{\alpha}^{-1} \kappa\mu h T_{\mathtt{m}} \\ & + \beta b_h \tilde{\alpha}^{-2} (cr(1 + \beta\alpha^M) \|\chi_0(t_\ell)\|^{[0,k]} \\ & + \beta b_h \tilde{\alpha}^{-1} cr(1+\beta) \|\chi_0(t_\ell)\|^{[0,k]} \\ & + \beta\tilde{\alpha}^{-1} T_{\mathtt{m}} h\kappa \|\chi_0(t_\ell)\|^{[0,k]} \\ & \leq \beta\alpha^k (1+\gamma) \max_{j\in(0,1)} \{|\chi_j(0)|\} \\ & + \beta\tilde{\alpha}^{-1} (1+\gamma)(2b_h + hT_{\mathtt{m}})\delta_d \\ & + \beta\tilde{\alpha}^{-1} (1+\gamma)\kappa\mu(b_h + hT_{\mathtt{m}}). \end{aligned}$$

Consider now the i^{th} vehicle with the trajectories in (18). As before, exploiting (9), one gets

$$\begin{aligned} |\chi_i(t_k)| \; & \leq \beta\alpha^k |\chi_i(0)| + \tfrac{\beta}{1-\alpha} \|w_i(t_\ell)\|^{[0,k]} \\ & + c\beta b_h r \tilde{\alpha}^{-1} \Big(\left(1 + \beta\alpha^M\right) \tilde{\alpha}^{-1} \\ & + (1+\beta) \Big) \max_{j\in\mathcal{I}_0^{i-1}} \left\{ \|\chi_j(t_\ell)\|^{[0,k]} \right\} \end{aligned} \tag{20}$$

At this point, noting that the term $u_{i-1}(t_k)$ and $f_i(t_k)$ verify

$$\begin{aligned} \|u_{i-1}(t_\ell)\|^{[0,k]} \; & \leq \|u_{i-2}^q(t_\ell)\|^{[0,k]} + \kappa \|\chi_{i-1}(t_\ell)\|^{[0,k]} \\ & + r\|\psi_{i-2}(t_\ell)\|^{[0,k^{\mathtt{M}}]} + (\kappa + r)\mu \\ & \leq D + \kappa \|\chi_{i-1}(t_\ell)\|^{[0,k]} + r\|\psi_{i-2}(t_\ell)\|^{[0,k^{\mathtt{M}}]} \\ & + (\kappa + r)\mu, \\ \|f_i(t_\ell)\|^{[0,k]} \; & \leq (2b_h + hT_{\mathtt{m}})\delta_d + T_{\mathtt{m}} h \|u_{i-1}(t_\ell)\|^{[0,k]} \end{aligned}$$

with D the quantizer range, one gets, for the disturbance $w_i(t_k)$ that

$$\begin{aligned} \|w_i(t_\ell)\|^{[0,k]} \leq & (2b_h + hT_{\mathtt{m}})\delta_d + T_{\mathtt{m}} h \Big(D + \kappa \|\chi_{i-1}(t_\ell)\|^{[0,k]} \\ & + r\|\psi_{i-1}(t_\ell)\|^{[0,k^{\mathtt{M}}]} + (\kappa + r)\mu \Big) \\ & + hT_{\mathtt{m}} b_h (\kappa + r)\mu. \end{aligned} \tag{21}$$

Combining (20) and (21) and exploiting (9) yields

$$\begin{aligned} & |\chi_i(t_k)| \leq \beta\alpha^k |\chi_i(0)| \\ & + \beta\tilde{\alpha}^{-1} h T_{\mathtt{m}} (\kappa \|\chi_{i-1}(t_\ell)\|^{[0,k]} + r\|\psi_{i-2}(t_\ell)\|^{[0,k^{\mathtt{M}}]}) \\ & + \beta\tilde{\alpha}^{-1} \left(hT_{\mathtt{m}} D + (2b_h + hT_{\mathtt{m}})\delta_d\right) \\ & + \beta\mu\tilde{\alpha}^{-1} (hT_{\mathtt{m}} + b_h)(\kappa + r) \\ & + \beta b_h r \tilde{\alpha}^{-1} (1 + \beta\alpha^M) \tilde{\alpha}^{-1} \|\psi_{i-1}(t_\ell)\|^{[0,k^{\mathtt{M}}]} \\ & + \beta b_h r \tilde{\alpha}^{-1} (1+\beta) \|\psi_{i-1}(t_\ell)\|^{[0,k^{\mathtt{M}}]} \\ & \leq \beta\alpha^k |\chi_i(0)| + \beta\tilde{\alpha}^{-1} hT_{\mathtt{m}} D \\ & + \beta(2b_h + hT_{\mathtt{m}})\delta_d \tilde{\alpha}^{-1} \\ & + \beta\tilde{\alpha}^{-1} \mu (hT_{\mathtt{m}} + b_h)(\kappa + r) \\ & + \beta b_h r \tilde{\alpha}^{-1} (1 + \beta\alpha^M) \tilde{\alpha}^{-1} c \max_{j\in\mathcal{I}_0^{i-1}} \left\{ \|\chi_{i-1}(t_\ell)\|^{[0,k]} \right\} \\ & + \beta b_h c r \tilde{\alpha}^{-1} (1+\beta) \max_{j\in\mathcal{I}_0^{i-1}} \left\{ \|\chi_{i-1}(t_\ell)\|^{[0,k]} \right\} \\ & + \beta b_h \tilde{\alpha}^{-1} \left(hT_{\mathtt{m}}(\kappa + cr)\right) \max_{j\in\mathcal{I}_0^N} \left\{ \|\chi_j(t_\ell)\|^{[0,k]} \right\}. \end{aligned}$$

By definition of (14), one has

$$\begin{aligned} |\chi_i(t_k)| \; & \leq \beta\alpha^k |\chi_i(0)| + \gamma \max_{j\in\mathcal{I}_0^{i-1}} \left\{ \|\chi_j(t_\ell)\|^{[0,k]} \right\} \\ & + \beta\tilde{\alpha}^{-1} b_h h T_{\mathtt{m}} D + \beta\tilde{\alpha}^{-1} b_h (2b_h + hT_{\mathtt{m}})\delta_d \\ & + \beta\tilde{\alpha}^{-1} \mu (hT_{\mathtt{m}} + b_h)(\kappa + r). \end{aligned}$$

As for all $l \in \mathcal{I}_0^{i-1}$,

$$\begin{aligned} |\chi_l(t_k)| \; & \leq \beta\alpha^k \textstyle\sum_{j=0}^{l} \gamma^j \max_{j\in\mathcal{I}_0^l} \{|\chi_j(0)|\} \\ & + \beta\tilde{\alpha}^{-1} \textstyle\sum_{j=0}^{l} \gamma^j \Big(hT_{\mathtt{m}} D + (hT_{\mathtt{m}} + b_h)(\kappa + r)\mu \Big) \\ & + \beta\tilde{\alpha}^{-1} \textstyle\sum_{j=0}^{l} \gamma^j (2b_h + hT_{\mathtt{m}})\delta_d \end{aligned}$$

with γ in (14), one gets, for all $i \in \mathcal{I}_0^N$

$$\begin{aligned} |\chi_i(t_k)| \; & \leq \beta\alpha^k \textstyle\sum_{j=0}^{i} \gamma^j \max_{j\in\mathcal{I}_0^i} \{|\chi_j(0)|\} \\ & + \beta\tilde{\alpha}^{-1} \textstyle\sum_{j=0}^{i} \gamma^j \Big((hT_{\mathtt{m}} D + (hT_{\mathtt{m}} + b_h)(\kappa + r)\mu \Big) \\ & + \beta\tilde{\alpha}^{-1} \textstyle\sum_{j=0}^{i} \gamma^j (2b_h + hT_{\mathtt{m}})\delta_d. \end{aligned}$$

As $\gamma \in (0,1)$, one gets $\sum_{j=0}^{i} \gamma^j \leq (1-\gamma)^{-1}$. Therefore, by taking the max operator, the following inequality holds true

$$\begin{aligned} \max_{i\in\mathcal{I}_0^N} \{|\chi_i(t_k)|\} \leq \; & \beta(1-\gamma)^{-1} \alpha^k \max_{i\in\mathcal{I}_0^N} \{|\chi_i(0)|\} \\ & + \vartheta_\mu + \vartheta_d \delta_d. \end{aligned}$$

Accordingly, pSS is proved (Def. 2.1) as, in particular: (i) follows setting for all $\varepsilon > 0$, $\alpha_\varepsilon = \frac{\varepsilon(1-\gamma)}{\beta\alpha}$ and ϑ_μ as in (15); (ii) holds as (22) implies that, for $d_i \equiv 0$ (and hence $\delta_d = 0$), $|\chi_i(t_k)| \to \vartheta_\mu$ and hence $|\chi_i(t_k)|_{\mathcal{B}_\mu} \to 0$. Finally, fixing $\beta_d(m,s) = \beta(1-\gamma)^{-1}\alpha^s m$ and $\rho_d(s) = \vartheta_d s$ with ϑ_d as in (15), DSS follows (Def. 2.2).